JAAS

ROYAL SOCIETY OF CHEMISTRY

PAPER

View Article Online
View Journal | View Issue

Cite this: *J. Anal. At. Spectrom.*, 2022, **37**, 783

New methods for determination of the mass-independent and mass-dependent platinum isotope compositions of iron meteorites by MC-ICP-MS†

Graeme M. Poole, *[abc] Roland Stumpf[a] and Mark Rehkämper [a]

Improved methods are presented for the separation of platinum from iron meteorites and subsequent analyses of both mass-independent and mass-dependent Pt isotope compositions of iron meteorites by multiple collector ICP-MS. The procedures are optimised for sample throughput and feature improvements in yield and the reduction of constituents that produce spectral interferences and matrix effects. The performance of the methods is demonstrated by replicate analyses of terrestrial reference materials and eight iron meteorites from the IC and IVB groups. The pilot iron meteorite analyses confirm previous work, which demonstrates that the Pt isotope compositions of iron meteorites are particularly sensitive to alteration by neutron capture reactions induced by exposure to galactic cosmic rays (GCR). It is shown that the mass-independent Pt isotope data obtained with the new methods are suitable for accurate correction of correlated cosmogenic isotope effects for other isotope systems in the same sample aliquots. The methods for the measurement of mass-dependent Pt isotope compositions (δ^{198}Pt) employ a robust double spike approach. The accurate determination of δ^{198}Pt values for iron meteorites requires, however, that possible cosmogenic isotope effects from GCR exposure are monitored and appropriately corrected on a sample aliquot specific basis. A robust approach for such corrections using the mass-independent Pt isotope data collected with the new methods is shown to provide accurate results for iron meteorites with variable compositions and GCR exposure histories. Initial results obtained for eight IC and IVB iron meteorites reveal both within- and between-group variations in δ^{198}Pt values, which indicate that such analyses may provide novel constraints for studies of planetary processes.

Received 30th December 2021
Accepted 10th March 2022

DOI: 10.1039/d1ja00468a

rsc.li/jaas

Introduction

In recent years, platinum isotopes have gained increasing importance in cosmochemistry, with several studies focusing on Pt isotope variations of cosmogenic origin in iron meteorites.[1,2] Galactic cosmic rays (GCR) are known to cause effects in the isotopic compositions of meteorites *via* spallation and neutron capture reactions, with Pt isotopes particularly susceptible to the latter.[1,3] With the better precision afforded by improvements in sample preparation and mass spectrometry methods, neutron capture reactions have been found to affect many isotope systems in iron meteorites, such as the short-lived Hf–W and Pd–Ag decay systems, as well as the isotope compositions of Mo, Ru and Os.[4–9] Such GCR effects can overprint other isotope effects of interest, such as radiogenic or nucleosynthetic isotope anomalies, and therefore must be corrected in order to obtain accurate "pre-exposure" data for the isotope system of interest. To do so, an isotope system that solely records GCR effects can be used as an *in situ* neutron dosimeter. In combination with the lack of resolvable nucleosynthetic Pt isotope anomalies,[2,10] the susceptibility of Pt isotopes to GCR effects render them a well-suited, and increasingly applied, system for use as *in situ* neutron dosimeters for correcting the isotopic data of other elements for GCR exposure.[5–7,11]

The susceptibility of the different Pt isotopes to GCR effects, and any variations in the isotope ratios these create, are not constrained by the relative masses of the isotopes, and hence the isotope variations are referred to as *mass-independent*. In contrast, variations in *mass-dependent* isotope compositions arise from physicochemical processes that fractionate isotope abundances, and hence ratios, based on differences in atomic mass. While there have been numerous investigations into mass-independent Pt isotope effects in iron meteorites, mass-dependent Pt isotope variations have yet to be fully explored,

[a]*Department of Earth Science and Engineering, Imperial College London, London SW7 2AZ, UK. E-mail: graeme.poole@nhm.ac.uk*

[b]*School of Earth Sciences, University of Bristol, Bristol BS8 1RJ, UK*

[c]*Imaging and Analysis Centre, Natural History Museum, London SW7 5BD, UK*

† Electronic supplementary information (ESI) available. See DOI: 10.1039/d1ja00468a

with only limited previous investigations.[10] Mass-dependent isotope fractionations for other elements have previously been studied to investigate processes in planetary bodies. For instance, planetary differentiation and core formation have been explored using Cr, Mo, Si and other isotope systems.[12–14] Platinum is a highly siderophile element with relatively high concentrations of up to about 50 μg g^{-1} in iron meteorites. Therefore, Pt isotopes offer a potentially useful tool to improve understanding of the processes and conditions relevant for the formation of iron meteorites and their parent bodies.

Here, we present new and improved analytical methods for studies of Pt isotopes in iron meteorites. To this end, we developed a more efficient separation procedure for Pt that can be used for both mass-independent and mass-dependent isotope studies. This method, combined with the isotopic analyses by multiple collector inductively coupled plasma mass spectrometry (MC-ICP-MS), is optimised for sample throughput to enable *in situ* neutron dosimetry for use in correcting data for other isotope systems disturbed by (mass-independent) GCR effects in the same samples. It can also be applied to help build a database of dosimetry information and to quantify the range of offsets from the terrestrial Pt isotope composition that GCR effects generate in different iron meteorite groups. For mass-dependent Pt isotope studies, we have developed an optimised analytical procedure that applies a Pt double-spike and uses the *in situ* dosimetry to remove the mass-independent (GCR) effects from the data for each specific sample and obtain accurate mass-dependent Pt isotope fractionations. As such, the methods are suitable for future high-precision Pt isotope studies of iron meteorites that investigate planetary processes, such as accretion, core formation and core crystallisation.

Methods

Reagents and materials

All sample preparation was performed in ISO class 4 laminar flow hoods in an ISO class 6 clean room at the MAGIC Laboratories at Imperial College London. To avoid any cross-contamination with the double spike, laboratory work for mass-independent and mass-dependent isotope analyses took place in separate flow hoods, using separate reagents and laboratory equipment. Concentrated HNO_3 (15 M), 6 M HCl and concentrated HCl (11 M) were purified in-house by sub-boiling distillation in quartz and PFA stills, respectively. Trace element grade Optima HBr (8 M) and Optima $HClO_4$ (12 M) were purchased from Fischer Scientific. All necessary dilutions were made using H_2O purified to >18 MΩ cm quality by a Millipore Academic system. Savillex PFA vials were used for sample handling, and were cleaned sequentially in 8 M HNO_3, 6 M HCl and dilute distilled acids (HNO_3 and HCl). Prior to use, the vials received a final cleaning by refluxing with a solution of distilled 6 M HCl.

Alfa Aesar 99% *n*-heptane was pre-cleaned using liquid–liquid extraction as outlined previously.[15] Herein, approximately 40 ml of heptane and 20 ml 6 M HCl were shaken together for 30 seconds in a 90 ml Savillex beaker and then left to stand for 3 minutes to allow for phase separation. Following this, the beaker was shaken again and allowed to stand for a further three minutes. The heptane was then carefully pipetted into a clean beaker and the entire cleaning process was repeated twice more.

Samples

This investigation used aliquots of iron meteorite solutions from a companion study (for continuity, the same sample numbers are used).[16] Specifically, eight iron meteorites from the IC and IVB groups, obtained from the Natural History Museum, London, were analysed. Iron meteorites are classified into groups based on the chemical compositions, whereby all meteorites from an individual group are derived from a single parent body. The IC and IVB groups were selected here due to (i) the ready availability of meteorites from these groups and (ii) the range of chemical compositions displayed by the meteorites within each group.

The robustness and reproducibility of the Pt separation procedure and the MC-ICP-MS Pt isotope measurements were routinely evaluated by repeated analyses of terrestrial standard reference materials. The NIST SRM (standard reference material) 129c High-Sulphur Steel was chosen for this purpose due to a major element composition that is somewhat similar to iron meteorites, with a high S content of about 2%. For analysis, the SRM was doped with a solution of SRM IRMM-010 Pt prior to digestion, to approximate the Pt concentrations of the iron meteorites, and then processed through the full digestion and chemical separation procedure and analysed together with the samples. In addition, a second in-house Pt standard solution, denoted Pt-α, was analysed *versus* IRMM-010 Pt to monitor data quality.

Sample preparation

The iron meteorites were prepared for analysis as described in the companion study.[16] Briefly, the samples were sequentially leached, at room temperature, in 0.5 M HBr, 6 M HCl and modified aqua regia (prepared from 6 M HCl and 15 M HNO_3, 3 : 1), to remove the outer surface and any terrestrial contamination. The leached samples were then submersed in distilled ethanol, dried and weighed. Following this, the samples, and NIST SRM 129c, were fully digested in modified aqua regia on a hotplate at 100–140 °C.

Platinum double spike preparation and calibration

To accurately determine *natural* mass-dependent isotope variations of samples *via* mass spectrometry, the instrumental mass-dependent isotope fractionation (IMF) must be corrected for. The double-spike technique, whereby two artificially enriched isotopes are mixed with the sample and used as a tracer for the IMF, provides the most accurate approach for obtaining such data with the precision required to resolve mass-dependent isotope variations in planetary samples (typical variations of 0.1–1 parts per 1000).

In this study, the double spike technique was used for the acquisition of mass-dependent Pt isotope data. For preparation

of the Pt double spike, enriched single isotopes of ^{198}Pt and ^{196}Pt were obtained from Isoflex USA in the form of Pt wire and digested in aqua regia. Based on double spike toolbox calculations,[17] the Pt double spike was gravimetrically prepared by mixing the ^{198}Pt and ^{196}Pt single spike solutions to produce a mixture with a ratio of ^{198}Pt/^{196}Pt ≈ 2.64.

The ^{198}Pt–^{196}Pt double spike composition was calibrated in two steps. Initial isotopic analyses applied external normalisation to admixed Ir for correction of the instrumental mass bias. An Ir-doped solution of IRMM-010 Pt was first analysed by MC-ICP-MS. The Pt isotope ratios of these runs were corrected for instrumental mass bias by both internal and external normalisation to ^{196}Pt/^{194}Pt and ^{193}Ir/^{191}Ir, respectively. The reference ratio $(^{193}Ir/^{191}Ir)_{Ref}$ employed in this procedure was empirically optimised to provide the best possible agreement between the isotope ratios normalised to Pt and Ir. This was followed by concentration-matched runs of the Ir-doped Pt double spike solution. In these analyses, the Pt isotope ratios were corrected for instrumental mass bias by external normalisation relative to the empirically optimised $(^{193}Ir/^{191}Ir)_{Ref}$ ratio from the previous IRMM-010 Pt runs. These measurements provided a provisional isotope composition for the ^{198}Pt–^{196}Pt double spike. In a second step, multiple mixtures of the Pt double spike and IRMM-010 Pt were prepared and analysed, whereby the mixtures had ratios of spike-derived to natural Pt (S/N ratios) of about 0.8 to 1.2.[18] A least squares approach was then applied using the Pt isotope data acquired for the mixtures, to define a marginally altered but optimised Pt double spike composition (Fig. 1).

Ion-exchange chromatography

Separation of Pt from the samples prior to both mass-independent and mass-dependent Pt isotope analyses was achieved with an anion-exchange chromatography procedure (Table 1). The single-column protocol, adapted from ref. 19 and 20, is optimised for efficient sample throughput. For mass-independent Pt isotope analyses, 30–100 mg of meteorite (~1000 ng Pt) were loaded onto the columns for each sample. For mass-dependent isotope analyses, 20–60 mg of meteorite (~600 ng natural Pt) were processed for each sample and prior to the separation chemistry, the sample solutions were mixed and equilibrated with the Pt double spike by refluxing on a hotplate for at least 24 hours.

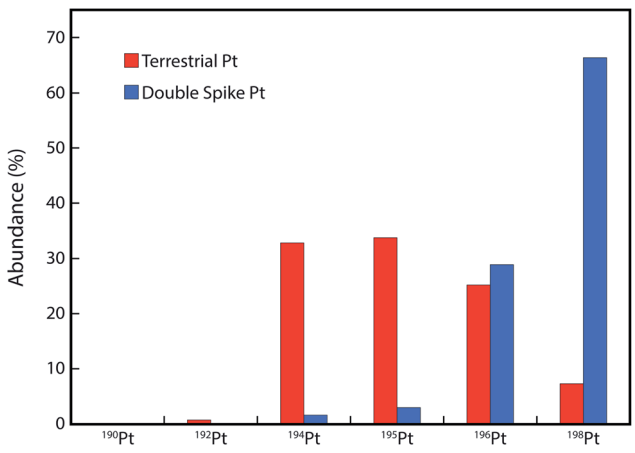

Fig. 1 Isotope composition of the new ^{198}Pt–^{196}Pt double spike. Shown are the double spike Pt isotope abundances, calibrated as described in text (blue bars), in comparison with terrestrial Pt isotope abundances (red bars).

Table 1 Ion-exchange chemistry for separation of Pt from iron meteorites

Quartz column, 3 ml resin reservoir, 50 ml acid reservoir		
Resin: Bio-Rad AG1-X8, 200–400 mesh, chloride form (1 ml)		
Step	Resin volumes	Acid
Cleaning	1.5	8 M HNO_3[a]
	1.5	11 M HCl
	1	1 M HCl
Pre-condition resin	4	1 M HCl
Load sample	2–4	1 M HCl
Elute matrix (inc. Fe, Ni)	40	0.5 M HCl
Elute Ir, Os, Re, Pd	50	11 M HCl[a]
Elute and collect Pt	14	13.5 M HNO_3

[a] Step followed by rinse with 1 ml H_2O to prevent aqua regia forming in resin during next step.

Following the full separation and clean-up chemistry, the purified Pt fractions typically had Os/Pt and Hg/Pt ratios of less than 1×10^{-5}. The procedural blank of the full sample preparation procedure was routinely monitored and ranged from 10–50 pg Pt. Considering that samples with ~1000 ng Pt were typically processed, the blank contribution to the total Pt analysed was negligible at <0.05‰. Total Pt yields were consistently 80–95%. This represents an improvement compared to previous procedures for Pt separation from iron meteorites, with reported yields of 50–70% (ref. 21) and ~70% Pt (ref. 22).

Elution of Pt with nearly concentrated (13.5 M) HNO_3 can cause decomposition of the ion-exchange resin and subsequent release of organic compounds. Consequently, the resin cannot be re-used and fresh resin was taken for every procedure. As all Pt is eluted from the columns in this final step of the procedure, any resin decomposition will have no impact on Pt yields.

However, the released organic compounds can have a detrimental impact on the quality of isotope analyses by MC-ICP-MS (*e.g.*, ref. 23). To mitigate such effects, a published method,[15] which employs liquid–liquid extraction with *n*-heptane, was employed to remove organic compounds from the eluate prior to the MC-ICP-MS analyses. The extraction procedure encompassed the following steps: (i) 10 ml pre-cleaned *n*-heptane were added to the eluate and shaken in a Savillex beaker for 30 seconds and then rested for 3 minutes. (ii) The shaking–resting was repeated a further two times. (iii) The organic phase was carefully removed with a pipette. (iv) The entire *n*-heptane procedure (steps i to iii) was then repeated. (v) After the organic phase was removed for the second time, any residual heptane was allowed to evaporate at ambient temperature in a laminar flow hood for 30–60 minutes.

Finally, the Pt fractions were dried down with a mixture of 15 M HNO_3 and 12 M $HClO_4$ to volatilise any remaining Os (as OsO_4), before being dissolved in 0.5 M HCl ready for MC-ICP-MS analysis.

Mass spectrometry

All isotope measurements were performed at the Imperial College London MAGIC Laboratories with a Nu Instruments Nu Plasma HR MC-ICP-MS. Sample introduction utilised a Cetac autosampler and a Nu Instruments DSN-100 desolvation system equipped with Micromist crossflow nebulisers with uptake rates of ~140 μl min^{-1}. Typical sensitivity for Pt, measured by Faraday cups with 10^{11} Ω resistors, was 180–210 V (μg^{-1} ml^{-1}), resulting in ^{196}Pt ion beams of 6–7 V for solutions with ~100 ng ml^{-1} natural Pt. All analyses utilised 3 blocks with 20 integrations of 5 seconds each. Each block was preceded by a 30 second on-peak baseline measurement while the ion beam was deflected by the electrostatic analyser.

Determination of mass-independent Pt isotope variations. The data for mass-independent isotope analyses were acquired by static multiple collection with the Faraday cups of the instrument. The cup configuration (Table 2) enabled simultaneous measurement of the ion beams of ^{192}Pt, ^{194}Pt, ^{195}Pt, ^{196}Pt, ^{198}Pt, as well as ^{188}Os, ^{200}Hg and ^{191}Ir, in a single cycle. Due to the very low abundance of ^{190}Pt (0.01%), adequate measurements of this isotope are unattainable with the current methods. Isobaric interferences from Os and Hg were corrected using ^{188}Os and ^{200}Hg as interference monitors, respectively, and published isotopic abundances.[24]

To obtain mass-independent isotope compositions, all mass-dependent isotope effects of natural and instrumental origin must be corrected. This is best achieved using internal normalisation, which fixes a particular Pt isotope ratio to the terrestrial value. Two separate internal normalisation schemes were employed here, with normalisation to both $^{198}Pt/^{195}Pt = 0.216277$ and $^{196}Pt/^{195}Pt = 0.748446$, using the exponential law.[25–27] Since these ratios have isobaric interferences (Hg on ^{196}Pt and ^{198}Pt), an iterative procedure was used to subtract these effects from the normalisation ratios.

Data for samples are reported in ε^{i}Pt notation (eqn (1)), calculated relative to the mean of several bracketing runs of an IRMM-010 Pt solution, made up to closely match (to within 5%) the Pt concentration of the samples (~100 ng g^{-1}):

$$\varepsilon^{i}\mathrm{Pt} = \left(\left[\frac{\left({}^{i}\mathrm{Pt}/{}^{x}\mathrm{Pt}\right)_{\mathrm{sample}}}{\left({}^{i}\mathrm{Pt}/{}^{x}\mathrm{Pt}\right)_{\mathrm{standard}}}\right] - 1\right) \times 10^{4} \quad (1)$$

Here the isotope ^{x}Pt is identical to the isotope that is used in the denominator of the normalising ratio. In the following, an $\varepsilon^{i}Pt_{(y/x)}$ nomenclature is adopted, where the ratio $^{i}Pt/^{19x}Pt$ is normalised to $^{19y}Pt/^{19x}Pt$; for example, $\varepsilon^{194}Pt_{(8/5)}$ stands for $^{194}Pt/^{195}Pt$ normalised to $^{198}Pt/^{195}Pt$ and given in ε notation relative to terrestrial Pt, in parts per ten thousand.

Determination of mass-dependent Pt isotope variations. As the natural abundances of ^{190}Pt and ^{192}Pt are very low (0.01% and 0.78%, respectively), the four isotopes selected for the Pt double spike data reduction were ^{194}Pt, ^{195}Pt, ^{196}Pt and ^{198}Pt. The simultaneous collection of the ^{194}Pt, ^{195}Pt, ^{196}Pt, ^{198}Pt, ^{200}Hg and ^{193}Ir ion beams (Table 2) enabled the measurement of the 'raw' $^{195}Pt/^{194}Pt$, $^{196}Pt/^{194}Pt$ and $^{198}Pt/^{194}Pt$ ratios, with all further data reduction carried out offline, after the measurements, using a spreadsheet-based iterative approach.[28–30]

Since the double spike is calibrated relative to the IRMM-010 Pt reference material, any variations in mass-dependent Pt isotope compositions calculated using the double-spike are determined relative to the composition of IRMM-010 Pt. Following convention, such variations are reported in δ-notation, based on variations in the $^{198}Pt/^{194}Pt$ ratio:

$$\delta^{198}\mathrm{Pt} = \left(\left[\frac{\left({}^{198}\mathrm{Pt}/{}^{194}\mathrm{Pt}\right)_{\mathrm{sample}}}{\left({}^{198}\mathrm{Pt}/{}^{194}\mathrm{Pt}\right)_{\mathrm{standard}}}\right] - 1\right) \times 10^{3} \quad (2)$$

The δ^{198}Pt values are thereby calculated relative to the mean results obtained for several bracketing runs of the IRMM-010 Pt reference material to which Pt double spike had been admixed. The double spiked IRMM-010 Pt solutions were made up to closely match both the total Pt concentrations (of ~100 ng g^{-1}) and the S/N ratios of the samples.

Resolving mass-dependent and mass-independent Pt isotope effects

The double spike data reduction determines the δ^{198}Pt value of a sample, based on the assumption that the isotopic difference between the sample and a standard reference material that represents $\delta^{198}Pt = 0$ (here represented by IRMM-010 Pt) is solely the result of mass-dependent isotope fractionation. However, when samples also host mass-independent isotope effects, biased results will be obtained for the mass-dependent isotope fractionation between sample and standard and hence the δ^{198}Pt values of the sample, unless corrections are applied to resolve the mass-dependent and mass-independent isotope effects (*e.g.*, ref. 18).

Platinum isotopes in iron meteorites are known to exhibit mass-independent anomalies from exposure to GCR.[1,3] Hence, analyses of such meteorites to determine mass-dependent Pt isotope fractionations (δ^{198}Pt) using the double spike method must accurately account for mass-independent isotope effects. One approach to achieve this would be to model and remove the mass-independent contribution to the δ^{198}Pt value determined

Table 2 Faraday cup configuration for mass-independent and mass-dependent Pt isotope measurements on the Nu Plasma HR MC-ICP-MS

Faraday cup	L5	L4	L3	L2	L1	Ax	H1	H2	H3	H4	H5	H6
Mass-independent			188		191	192		194	195	196	198	200
Mass-dependent							193	194	195	196	198	200

by the double spike measurements. It was previously shown that such an approach can accurately remove the effects of nucleosynthetic isotope anomalies from analyses to determine the mass-dependent Mo isotope compositions of iron meteorites.[14,31] However, this method can only provide accurate results if the magnitude and isotopic patterns of the mass-independent isotope effects are known with a high degree of confidence. For Mo, the nucleosynthetic isotope anomalies are well understood and so the approach is valid. However, whilst models of GCR effects on Pt isotopes in iron meteorites yield useful first order estimates,[1,3] significant discrepancies remain between measured and modelled data. These discrepancies have been attributed to limitations and uncertainties in the models, namely with respect to shielding depths, exposure ages and differences in chemical compositions.[1,2] Therefore, this approach is much less appropriate for the Pt isotope system.

An alternative approach to remove the effects of mass-independent isotope anomalies on the determination of mass-dependent isotope fractionations, involves use of the independently determined mass-independent isotope effects of each sample in the double spike data reduction. This approach was previously applied to determine mass-dependent Mo, Ru and Sr isotope data for meteorites[14,32,33] and it is used here for Pt. For Pt, the approach entails that the internally normalised mass-independent Pt isotope data for the unspiked sample (determined relative to IRMM-010 Pt) are applied to define the δ^{198}Pt = 0 reference composition, rather than the composition of IRMM-010 Pt. The δ^{198}Pt value that is provided by the procedure then characterises only the mass-dependent isotope effects. The uncertainties associated with the mass-independent Pt isotope measurements were thereby propagated through all data reduction and correction procedures, which are further described below.

Results and discussion

Determination of mass-independent Pt isotope compositions

Standard solutions and reference materials. The typical ±2se within-run precision and the ±2sd between-run precision of the Pt isotope data for the four (or more) runs of the IRMM-010 Pt SRM that bracketed each sample analysis are summarised in Table 3. It is notable that the two normalisation procedures yield similar precisions, which most likely reflects that ^{194}Pt, ^{195}Pt and ^{196}Pt have similar isotope abundances of 32.9, 33.8 and 25.2%, respectively. For all ε^{i}Pt values, except ε^{192}Pt, the between-run and the within-run precision are very similar at about ±0.1 to ±0.2 ε, demonstrating the excellent performance of the procedures. However, for ε^{192}Pt the between-run precision is about a factor of 2 worse than the within-run precision. A similar observation was made by ref. 1 and attributed to the low abundance of ^{192}Pt (0.78%), which renders the measurements more susceptible to matrix effects than those of the other, far more abundant, isotopes.

A similar between-run precision to that obtained for the IRMM-010 Pt measurements was determined for replicate analyses of Pt-α solutions relative to IRMM-010 Pt (Table 3). In addition, comparable results were also obtained for multiple measurements of NIST SRM 129c, which was doped with IRMM-010 Pt and processed by digestion and the column chemistry. Furthermore, the analyses of both Pt-doped NIST SRM 129c and the Pt-α solution yielded terrestrial Pt isotope compositions for all normalisation schemes (Fig. 2 and ESI Table S1†).

Iron meteorites. The mass-independent Pt isotope compositions for the iron meteorites are shown in Table 4. For data internally normalised to ^{198}Pt/^{195}Pt, large variations in ε^{192}Pt$_{(8/5)}$ are observed, with values ranging from +55.15 ± 1.12 for Tlacotepec (IVB) to terrestrial or near-terrestrial isotope compositions for several IC meteorites. Similarly, there are clear excesses in ε^{194}Pt$_{(8/5)}$ and ε^{196}Pt$_{(8/5)}$, although these anomalies are generally about an order of magnitude smaller than the variations in ε^{192}Pt$_{(8/5)}$. The individual meteorite results also document significant variations within the two investigated iron meteorite groups. Similar patterns are observed when the Pt isotope data are normalised to ^{196}Pt/^{195}Pt, with clearly resolvable variations in ε^{192}Pt$_{(6/5)}$, ε^{194}Pt$_{(6/5)}$, and ε^{198}Pt$_{(6/5)}$. This is to be expected as the different normalisation schemes simply reflect different ways of correcting for the instrumental mass bias.

The purified Pt fractions of the iron meteorites typically had Os/Pt and Hg/Pt ratios of less than 1×10^{-5} and these were associated with maximum interference corrections of 350 ppm for ε^{192}Pt and 40 ppm for ε^{198}Pt. Molecular interferences (*e.g.*, from ^{152}Sm^{40}Ar on ^{192}Pt, ^{182}W^{16}O on ^{198}Pt) were also routinely monitored after the isotope analyses but these were sufficiently small to be completely negligible. The isotope ^{191}Ir was monitored as it can produce tailing effects on ^{192}Pt (*e.g.*, ref. 1). During the course of this study, the abundance sensitivity of the Nu Plasma HR MC-ICP-MS, measured on ^{237}U *versus* ^{238}U, was ~1 ppm. For the samples analysed here, the Ir/Pt ratios of the Pt fractions ranged from 0.002 to 0.1, which implies that tailing effects from ^{191}Ir impacted the ε^{192}Pt values by less than 0.2 ε-units. No corrections for the tailing effects were applied in this study, as the ε^{192}Pt data for iron meteorites typically had

Table 3 Between-run precision (±2sd) and typical within-run precision (±2se) of Pt isotope measurements for $n = 4$ bracketing IRMM-010 Pt SRM runs

	ε^{192}Pt$_{(8/5)}$[a]	ε^{194}Pt$_{(8/5)}$[a]	ε^{196}Pt$_{(8/5)}$[a]	ε^{192}Pt$_{(6/5)}$[b]	ε^{194}Pt$_{(6/5)}$[b]	ε^{198}Pt$_{(6/5)}$[b]
Between-run precision (±2sd)	2.25	0.15	0.12	2.26	0.19	0.35
Within-run precision (±2se)	1.13	0.12	0.08	1.17	0.15	0.25

[a] Normalised to ^{198}Pt/^{195}Pt = 0.216277 using the exponential law, $\varepsilon^{i}Pt = [(^{i}Pt/^{195}Pt)_{smp}/(^{i}Pt/^{195}Pt)_{std} - 1] \times 10^{4}$. [b] Normalised to ^{196}Pt/^{195}Pt = 0.748446 using the exponential law, $\varepsilon^{i}Pt = [(^{i}Pt/^{195}Pt)_{smp}/(^{i}Pt/^{195}Pt)_{std} - 1] \times 10^{4}$.

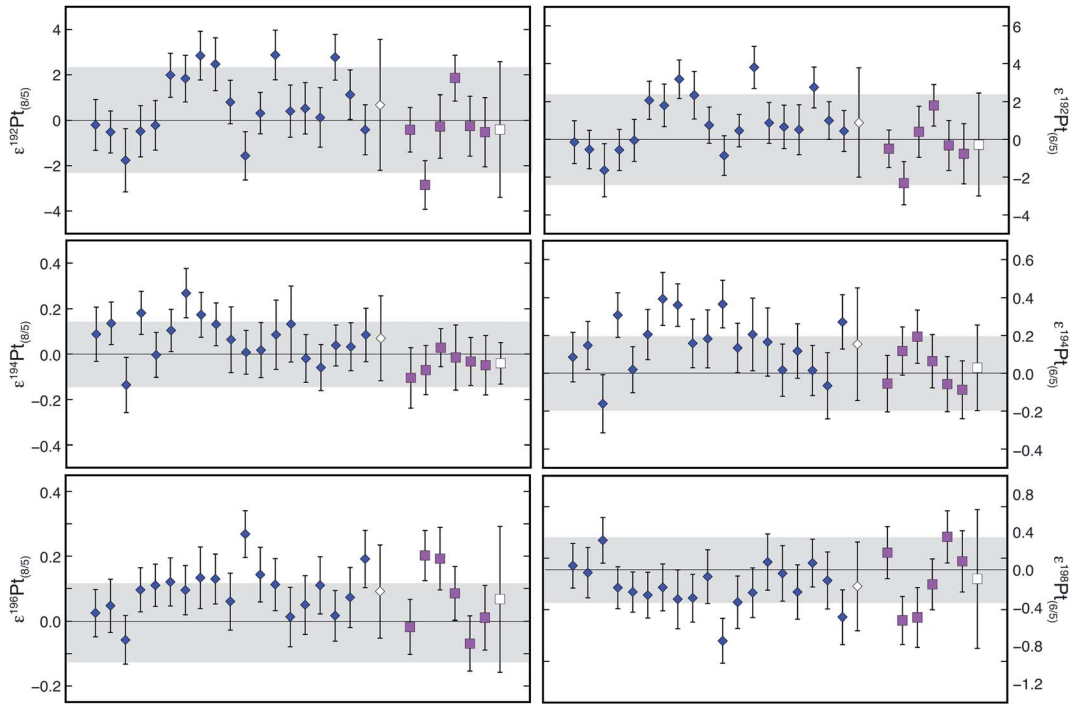

Fig. 2 Mass-independent Pt isotope data for terrestrial reference materials (diamonds = NIST SRM 129c doped with IRMM-010 Pt, squares = Pt-α, open symbols = mean) determined relative to bracketing runs of the IRMM-010 Pt SRM. Error bars denote the ±2se within-run precision; uncertainties of reported means are ±2sd. Grey-shaded area represents the typical between-run precision of the bracketing IRMM-010 Pt runs.

significantly larger analytical errors of about ±0.5 to ±2.2 ε-units (Table 4). Notably, our separation procedure produces Pt separates that have lower Ir/Pt ratios and which hence have less tailing effects on ^{192}Pt than other published methods. For instance, the Pt fractions separated from iron meteorites with the separation procedure of ref. 1 had Ir/Pt ratios of between 0.25 and 1.5, which would require tailing corrections for ε^{192}Pt of about 2 to 15 ε-units. Unlike previous methods (*e.g.*, ref. 2), our procedure produced Pt separates that have sufficiently low Ir/Pt ratios, such that a second clean-up column to further reduce Ir levels is not required. This single column procedure thereby significantly reduces the time needed for sample preparation, enabling an improved sample throughput.

During the iron meteorite analyses, attention was also paid to nebuliser uptake rates, as the presence of organic compounds that are released from the ion exchange resin by the 13.5 M HNO_3 used for Pt elution could cause fluctuations in flow-rate that may be detrimental to data quality. However, no such problems were encountered, which implies that the *n*-heptane extraction successfully removed problematic compounds.

Cosmogenic Pt isotope effects. Platinum isotopes were previously shown to be particularly susceptible to cosmogenic isotope effects from exposure to galactic cosmic rays (GCR)[3] and the mass-independent Pt isotope anomalies of iron meteorites analysed in this study show clear evidence of such effects. In detail, GCR exposure produces an excess in ^{196}Pt relative to ^{195}Pt and ^{198}Pt because ^{195}Pt captures thermal, epithermal and faster neutrons more efficiently than ^{196}Pt and ^{198}Pt.[1,3] The burnout of ^{195}Pt to produce ^{196}Pt, therefore, dominates the neutron capture effects recorded in isotope ratios between these three nuclides.

Table 4 Mass-independent Pt isotope compositions of the iron meteorites

Group	Sample	NHM BM[a]	N^b	$\varepsilon^{192}Pt_{(8/5)}{}^c$	$\varepsilon^{194}Pt_{(8/5)}{}^c$	$\varepsilon^{196}Pt_{(8/5)}{}^c$	$\varepsilon^{192}Pt_{(6/5)}{}^d$	$\varepsilon^{194}Pt_{(6/5)}{}^d$	$\varepsilon^{198}Pt_{(6/5)}{}^d$
IC	Arispe 3	2005,M11	4	11.80 ± 1.36	0.85 ± 0.13	0.55 ± 0.08	13.49 ± 1.11	1.44 ± 0.11	−1.64 ± 0.25
	Arispe 4	2005,M11	12	12.96 ± 0.45	0.97 ± 0.04	0.61 ± 0.04	15.15 ± 0.69	1.56 ± 0.05	−1.83 ± 0.11
	Bendego 1	1938,2656	3	−0.19 ± 0.88	0.85 ± 0.14	0.61 ± 0.16	2.66 ± 0.90	1.46 ± 0.05	−1.83 ± 0.48
	Bendego 2	1938,2656	4	2.45 ± 2.19	1.20 ± 0.19	0.96 ± 0.02	5.28 ± 2.20	2.23 ± 0.17	−2.87 ± 0.07
	Santa Rosa	1985,M291	5	0.99 ± 0.53	0.00 ± 0.10	0.31 ± 0.08	1.70 ± 0.34	0.24 ± 0.05	−0.65 ± 0.14
IVB	Cape of Good Hope	1985,M246	4	23.94 ± 1.49	1.18 ± 0.08	0.56 ± 0.08	25.62 ± 1.60	1.67 ± 0.08	−1.67 ± 0.25
	Santa Clara	1983,M27	6	15.48 ± 0.79	1.26 ± 0.19	0.71 ± 0.07	17.58 ± 0.89	1.99 ± 0.22	−2.12 ± 0.20
	Tlacotepec 1	1959,913	4	55.15 ± 1.12	2.11 ± 0.11	0.89 ± 0.06	57.75 ± 1.48	3.05 ± 0.15	−2.66 ± 0.17

[a] Natural History Museum, London, BM collection number. [b] Number of times sample analysed. [c] Normalised to $^{198}Pt/^{195}Pt = 0.216277$ using the exponential law, $\varepsilon^{i}Pt = [(^{i}Pt/^{195}Pt)_{smp}/(^{i}Pt/^{195}Pt)_{std} - 1] \times 10^4$. [d] Normalised to $^{196}Pt/^{195}Pt = 0.748446$ using the exponential law, $\varepsilon^{i}Pt = [(^{i}Pt/^{195}Pt)_{smp}/(^{i}Pt/^{195}Pt)_{std} - 1] \times 10^4$; uncertainties are 2se = $2\sigma/\sqrt{n}$, where n is the number of sample analyses.

Additionally, both ^{191}Ir and ^{193}Ir have large neutron capture cross sections and resonance integrals, and can efficiently capture neutrons with epithermal energies.[3] When ^{191}Ir and ^{193}Ir capture neutrons, they produce ^{192}Ir and ^{194}Ir, respectively. The latter nuclides are both unstable and β^- decay to generate excesses in ^{192}Pt and ^{194}Pt, of a magnitude that critically depends on the Ir/Pt ratio of the meteorite. The ^{194}Pt excess is thereby much less sensitive to the Ir/Pt ratio because this isotope is far more abundant than ^{192}Pt, with terrestrial abundances of 32.9 and 0.78%, respectively.

Notably, the observed Pt isotope anomalies of the iron meteorites (Table 4), are in good accord with the expected trends and the cosmogenic isotope systematics predicted by quantitative GCR models[3] (Fig. 3). Such models, however, provide only a first order prediction of the expected cosmogenic isotope effects and they were found to be inaccurate in some cases, most likely due to uncertainties and variations in exposure ages and chemical compositions.[1,2] Moreover, the models are only able to account for the shielding depths of meteorites with pre-exposure atmospheric radii of up to 120 cm. Nevertheless, the good agreement found between our meteorite data and the modelled trends lends credence to the quality of the Pt isotope results.

Our data are, furthermore, in good agreement with the results of previous iron meteorite analyses[1,11,21,22] with similar patterns of excesses for $\varepsilon^{192}Pt_{(8/5)}$, $\varepsilon^{194}Pt_{(8/5)}$, and $\varepsilon^{196}Pt_{(8/5)}$. However, care must be taken with such comparisons, as cm-scale variations in compositions and shielding depths across a meteorite can induce ε-level changes in ^{192}Pt abundances.[3,21] For instance, the $\varepsilon^{192}Pt_{(8/5)}$ value for our sample of Tlacotepec (55.15 ± 1.12) differs from a previous result of 58.6 ± 2.2 and this difference may reflect a separation in the pre-atmospheric shielding depth of only 3 cm or less.[1] Similarly, our analyses of Santa Clara yielded higher $\varepsilon^{194}Pt_{(8/5)}$ and $\varepsilon^{196}Pt_{(8/5)}$ values compared to those of ref. 1 and 21. However, the ratio of the excesses in $\varepsilon^{194}Pt_{(8/5)}$ *versus* $\varepsilon^{196}Pt_{(8/5)}$ are identical, suggesting that our sample of Santa Clara was more exposed to GCR, perhaps because it was situated closer to the meteoroid surface.

The neutron dosimetry afforded by precise mass-independent Pt isotope data of iron meteorites can be used to empirically correct the results obtained for other isotope systems, such as W, Mo, Ru and Pd, for GCR-induced isotope effects.[5–7,11] However, the observed variations in cosmogenic Pt isotope effects even for samples of the same meteorite and the known discrepancies between modelled and measured anomalies,[2] demonstrate that such corrections must be sample-specific to be accurate. This correction approach is illustrated in Fig. 4. In this figure, the Mo isotope data of the companion study[16] are plotted *versus* the Pt isotope compositions of this study, whereby both analyses were obtained for the same IC iron meteorite sample aliquots; also shown are additional results from the literature.[11,22,34] The observed variations in ε^{i}Mo and ε^{i}Pt correlate as expected for cosmogenic isotope effects[11,22] and a pre-exposure Mo isotope composition for the IC iron meteorite group can be obtained from the intercept at $\varepsilon^{196}Pt_{(8/5)} = 0$. In this case, a pre-exposure ε^{95}Mo of 0.40 ± 0.04 is obtained, in excellent accord with a previous result of 0.40 ± 0.03.[11]

These results demonstrate that our chemical and mass spectrometric techniques for the determination of mass-independent Pt isotope compositions can provide highly precise sample aliquot specific neutron dosimetry for iron meteorites, whilst utilising a less time-consuming and more effective sample preparation procedure in comparison to published methods.[1,2,19,20]

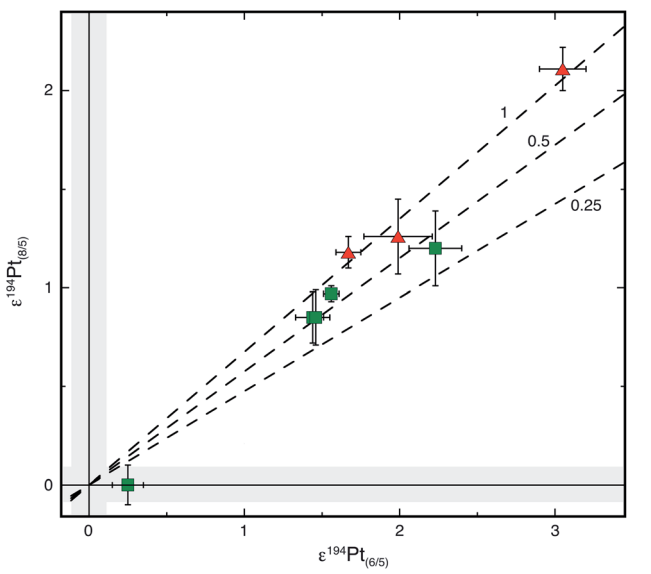

Fig. 3 Plot of $\varepsilon^{194}Pt_{(8/5)}$ *vs.* $\varepsilon^{194}Pt_{(6/5)}$ for all iron meteorites analysed (green squares = IC irons; red triangles = IVB irons). All data are mean values with uncertainties of 2se = 2sd/$\sqrt{n}$, where n = number of times sample analysed. Grey shaded area represents 2sd of bracketing IRMM-010 Pt SRM runs. Also shown are the cosmogenic Pt isotope trends predicted by modelling for Ir/Pt ratios of 1, 0.5 and 0.25.[3]

Determination of mass-dependent Pt isotope fractionation

Standard solutions and reference materials. To evaluate the precision and accuracy of the mass-dependent Pt isotope data,

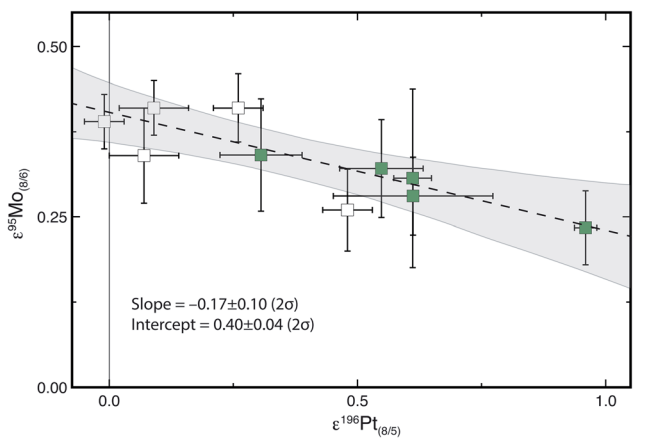

Fig. 4 ε^{95}Mo *vs.* $\varepsilon^{196}Pt_{(8/5)}$ for IC iron meteorites. Solid symbols = Pt data from this study and Mo data, normalised to ^{98}Mo/^{96}Mo, from companion study.[16] Open symbols = literature data.[11,22,34] A pre-exposure ε^{95}Mo for the IC group is obtained from the intercept at $\varepsilon^{196}Pt_{(8/5)} = 0$.

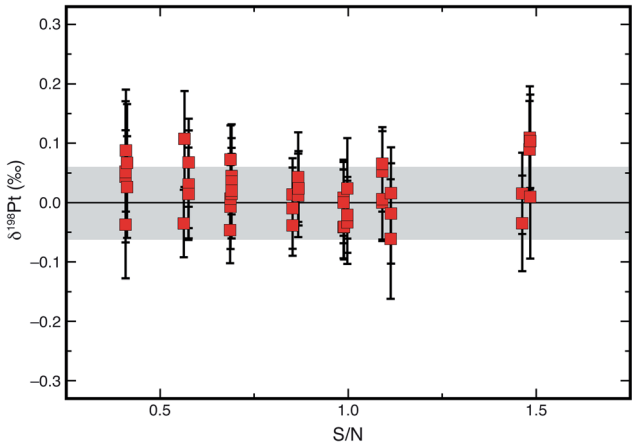

Fig. 5 δ^{198}Pt values of IRMM-010 Pt standard solutions with variable ratios of spike-derived Pt to natural Pt (S/N). The solutions were analysed relative to a solution with S/N = 0.84. The grey shaded area represents the typical between-run precision of the bracketing standard solutions. For solutions with S/N = 0.7 to 1.0, the uncertainties in δ^{198}Pt are a factor of ~1.5 better than for solutions with S/N outside this range.

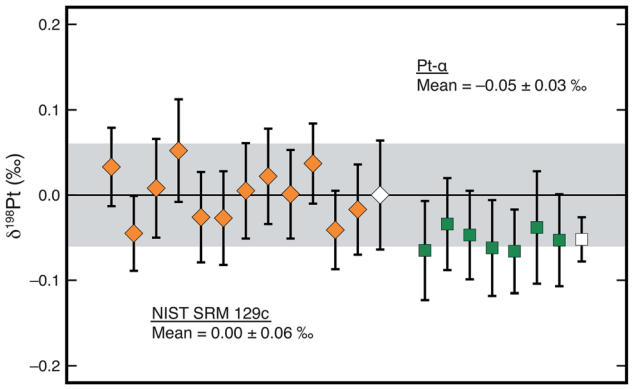

Fig. 6 δ^{198}Pt values of terrestrial standard reference materials (squares = NIST SRM 129c doped with IRMM-010 Pt, diamonds = Pt-α, open symbols = mean) determined relative to bracketing IRMM-010 Pt SRM runs. Error bars denote the ±2se within-run precision; uncertainties of reported means are ±2sd. Grey-shaded area represents the typical ±0.06‰ between-run precision of the bracketing IRMM-010 Pt standard solutions.

multiple IRMM-010 Pt solutions with variable S/N ratios were analysed (Fig. 5). These mixtures, with S/N of between about 0.4 and 1.5, were analysed relative to an IRMM-010 Pt solution with an optimised S/N = 0.84, as predicted by numerical error propagation.[17] The δ^{198}Pt data are about a factor of 1.5 more precise for solutions with S/N ratios of between 0.7 and 1.0, than for S/N <0.7 or >1.0.

Based on these results, samples were spiked to obtain S/N ≈ 0.84. This helps to ensure that there is no detrimental impact on data quality even if the actual spiking was slightly off because the sample Pt concentration was not characterised well, as long as the sample solution features an S/N ratio of between 0.7 and 1.0. The typical between-run reproducibility of bracketing runs of spiked IRMM-010 Pt solutions with ~100 ng ml^{-1} total Pt and S/N ≈ 0.84 was ±0.06‰ (2sd) for δ^{198}Pt, with a typical within-run δ^{198}Pt precision of ±0.05‰ (2se).

The robustness and reproducibility of the Pt separation procedure and MC-ICP-MS measurements were routinely evaluated by repeated analyses of terrestrial reference materials. To this end, NIST SRM 129c (High-Sulphur Steel) was mixed and equilibrated with the Pt double spike and IRMM-010 Pt, to prepare a solution that matched the Pt concentration and S/N of samples prior to ion-exchange chromatography. The analyses of this Pt-doped reference material relative to IRMM-010 Pt consistently yielded the correct isotope composition, with a mean result of δ^{198}Pt = 0.00 ± 0.06‰ (2sd; Fig. 6 and ESI Table S2†). Double-spiked aliquots of the Pt-α standard solution were also analysed against IRMM-010 Pt during each measurement session to monitor data quality. These analyses yielded a reproducible offset of δ^{198}Pt = −0.05 ± 0.03‰ for Pt-α relative to IRMM-010 Pt (Fig. 6 and ESI Table S2†).

Correction of δ^{198}Pt data for cosmogenic isotope effects. A graphical representation of the Pt double spike technique, with interest focused on determining the natural mass-dependent isotope fractionation of a sample relative to a reference material, is provided in the four-isotope plot of Fig. 7. The double spike composition, S, is known from the initial calibration of the double spike, while n is the composition of the standard reference material that anchors δ^{198}Pt = 0 (here IRMM-010 Pt). The isotope composition of the sample, N, differs from n as a result of the natural mass fractionation, α. The isotope composition of the mixture of sample and double spike, m, is determined by mass spectrometry. This differs from the true, unfractionated, isotope composition of the mixture, M, as a result of the instrumental mass bias, β.

In four-isotope space (Fig. 7), the points N, n and S lie on the same plane, P_n, while M, m and S lie on a second plane, P_m.

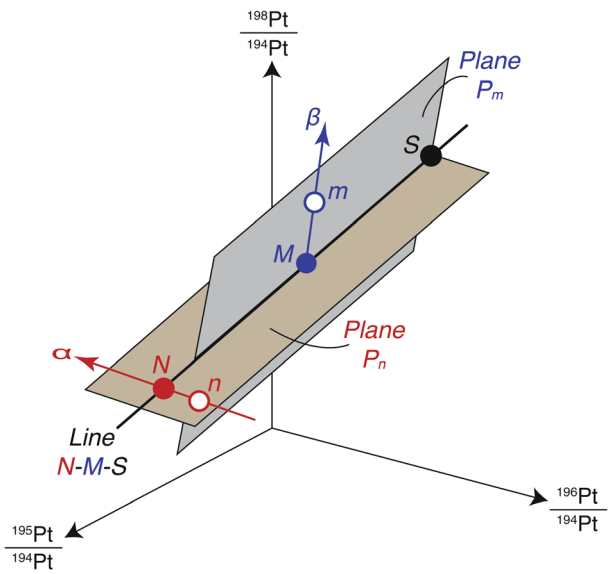

Fig. 7 Schematic of the Pt double spike technique in four-isotope space. Adapted from ref. 35.

These two planes intersect along the mixing line formed by *N*–*M*–*S*. From this mathematical framework, and inputting the parameters *n* and *S* as well as the measured value for *m*, an iterative approach is used to calculate *N*.

The double spike data reduction assumes that the isotopic difference between the sample (*N*) and the SRM (*n*) is solely the result of mass-dependent isotope fractionation. When iron meteorites host resolvable mass-independent (cosmogenic) Pt isotope anomalies (Table 4),[1,3] use of the SRM composition as *n* to determine *N* will produce biased results for the latter parameter and the associated δ^{198}Pt of the sample. Two measurements are required in this case. One measurement is for a spiked sample aliquot to determine *m*, whilst a second is needed for the unspiked sample to define the sample isotope composition *n*, which is then used in the double spike data reduction instead of the SRM composition.[17,18] For Pt, this entails using the previously measured internally normalised mass-independent Pt isotope ratios of the samples for *n*. Notably, the same ratios were previously used to define the cosmogenic Pt isotope anomalies of the samples, which are reported as ε^{i}Pt values relative to IRMM-010 Pt (Table 4). This approach of using internally normalised data for the unspiked measurements is commonly applied in studies of mass-dependent isotope fractionations of elements that also have mass-independent isotope effects (*e.g.*, Sr, Mo) due to the favourable error propagation and the internal consistency of the results.[14,33]

To investigate the robustness of the double spike data reduction, mass-independent isotope ratios that were internally normalised to both ^{198}Pt/^{195}Pt and ^{196}Pt/^{195}Pt were applied as the unspiked sample compositions (*n*). The results reveal that regardless of which internal normalisation scheme is used, the same value of *N* is always obtained. This reflects that *n* must lie on a mass-fractionation line with *N* irrespective of the normalisation scheme that is applied.[31] In the example of Tlacotepec shown in Table 5, use of either ^{198}Pt/^{195}Pt or ^{196}Pt/^{195}Pt for internal normalisation of the unspiked sample measurement yields two different *n* compositions, with ^{198}Pt/^{194}Pt ratios of 0.222690 and 0.222610, respectively. Application of these *n* compositions in the data reduction then yields identical (within uncertainty) *N* values of ^{198}Pt/^{194}Pt = 0.222691 and 0.222694, respectively. Issues arise, however, when δ^{198}Pt values are calculated from *N*. As the result obtained for *N* is the same, regardless of which normalisation scheme is used for the unspiked measurement, the calculation of δ^{198}Pt values relative to different *n* values generates different δ^{198}Pt results. For Tlacotepec, calculation of δ^{198}Pt relative to the two *n* compositions yields significantly different results of 0.00‰ and +0.38‰, respectively (Table 5).

This problem arises because all Pt isotopes that are monitored in the mass-independent isotope analyses (^{192}Pt, ^{194}Pt, ^{195}Pt, ^{196}Pt and ^{198}Pt) are altered by cosmogenic isotope effects. Consequently, Pt lacks an invariant isotope ratio that can be employed to constrain the absolute changes in isotope abundances that were produced by GCR exposure. Rather, use of internal normalisation in the mass-independent isotope measurements of samples fixes a particular Pt isotope ratio to the terrestrial value even if this has a cosmogenic isotope anomaly. The Pt isotope ratios determined from such analyses are therefore 'skewed' by mass-independent effects if the normalisation scheme employs an isotope ratio that differs significantly in a sample from the terrestrial value due to GCR exposure. As a consequence, the procedure generates different δ^{198}Pt values for the same sample, depending on which normalisation scheme is used for the unspiked measurement (*n*).

For consistency and to enable a meaningful comparison of δ^{198}Pt values that are determined for different iron meteorites, δ^{198}Pt is calculated in the following from *N* (which itself has been calculated using the unspiked composition *n*) relative to the fixed SRM isotope composition. For Tlacotepec, this leads to essentially identical (within uncertainty) δ^{198}Pt values of −0.21 and −0.19‰ for the two different normalisation schemes that were employed in the mass-independent isotope analyses (Table 5). The procedure of determining δ^{198}Pt from *N* relative to *n*, does, however, leave a small mass-independent contribution in the calculated δ^{198}Pt values. This mass-independent contribution to δ^{198}Pt cannot be rigorously quantified since the absolute Pt isotope abundances of unspiked iron meteorites, which have cosmogenic isotope anomalies, are insufficiently constrained by isotope measurements that employ internal normalisation.

It is possible, however, to estimate the magnitude of this remaining mass-independent contribution to δ^{198}Pt for samples that exhibit realistic mass-independent Pt isotope anomalies of less than 10 ε^{i}Pt (for ε^{194}Pt, ε^{195}Pt, ε^{196}Pt, ε^{198}Pt) and mass-dependent Pt isotope effects of less than 1‰ for δ^{198}Pt. With these constraints, modelling reveals that the remaining mass-independent contributions to δ^{198}Pt are always smaller than ±0.02‰, which is less than the best within-run 2se uncertainties that are reported here for the δ^{198}Pt values of samples (Table 6). As such, the remaining mass-independent contributions to δ^{198}Pt are essentially negligible and this validates the credibility of our approach.

Table 5 Results obtained for the Tlacotepec iron meteorite using the different correction procedures

	^{198}Pt/^{194}Pt		δ^{198}Pt (‰)	
Unspiked measurement data	*n*	*N*	*N* relative to *n*	*N* relative to SRM
Normalised to ^{198}Pt/^{195}Pt	0.222690	0.222691	+0.00	−0.21
Normalised to ^{196}Pt/^{195}Pt	0.222610	0.222694	+0.38	−0.19
SRM composition	0.222737	0.222665	−0.32	−0.32

Table 6 Platinum concentrations and mass-dependent isotope compositions of the iron meteorites

Group	Sample	N^a	Pt (μg g^{-1})^b	Ir/Pt^c	$\delta^{198}Pt_{(8/5)}$^{d} (‰)	$\delta^{198}Pt_{(6/5)}$^{e} (‰)	$\delta^{198}Pt_{(SRM)}$^{f} (‰)
IC	Arispe 3	5	18.7	0.59	−0.07 ± 0.03	−0.08 ± 0.03	−0.09 ± 0.01
	Arispe 4	5	18.9	0.59	−0.02 ± 0.03	−0.03 ± 0.03	−0.04 ± 0.02
	Bendego 1	5	11.80	0.02	0.31 ± 0.05	0.29 ± 0.04	0.29 ± 0.03
	Bendego 2	5	11.5	0.02	0.30 ± 0.05	0.31 ± 0.04	0.30 ± 0.04
	Santa Rosa	5	5.1	0.01	0.19 ± 0.04	0.17 ± 0.04	0.22 ± 0.04
IVB	Cape of Good Hope	6	30.1	1.05	−0.01 ± 0.03	−0.02 ± 0.03	−0.06 ± 0.02
	Santa Clara	7	23.1	0.78	−0.07 ± 0.04	−0.08 ± 0.04	−0.09 ± 0.02
	Tlacotepec 1	5	18.6	1.29	−0.21 ± 0.03	−0.19 ± 0.04	−0.32 ± 0.02

^{a} Number of times sample was analysed. ^{b} Pt concentrations determined by isotope dilution. ^{c} Ir/Pt ratios calculated using Ir data from *Catalogue of Meteorites* (2000) and references therein. ^{d} $\delta^{198}Pt_{(8/5)}$ values corrected for GCR effects using unspiked data normalised to $^{198}Pt/^{195}Pt$. ^{e} $\delta^{198}Pt_{(6/5)}$ values corrected for GCR effects using unspiked data normalised to $^{196}Pt/^{195}Pt$. ^{f} $\delta^{198}Pt_{(SRM)}$ values obtained if no corrections are applied to the data for GCR effects. Uncertainties are 2se = $2\sigma/\sqrt{n}$, where n is the number of times the sample was analysed.

If, for comparison, the SRM isotope composition is applied in the double spike data reduction as n to determine N, instead of the data from the unspiked measurement, a $\delta^{198}Pt$ value of −0.32‰ is determined for Tlacotepec (Table 5). Our approach therefore corrects the $\delta^{198}Pt$ value for a cosmogenic isotope effect of 0.11‰ or 0.13‰, depending on whether the unspiked data for Tlacotepec used $^{198}Pt/^{195}Pt$ or $^{196}Pt/^{195}Pt$ for internal normalisation, respectively. Notably, these corrections are in perfect agreement with a previous study, which showed that the $\delta^{198}Pt$ value determined for Tlacotepec with the double spike method was shifted by −0.13‰ due to exposure to GCR.[10]

Iron meteorites. The mass-dependent isotope compositions of the iron meteorites, in the form of $\delta^{198}Pt$ values, are summarised in Table 6 and Fig. 8. The $\delta^{198}Pt$ values corrected for cosmogenic isotope effects using data for the unspiked iron meteorites internally normalised to $^{198}Pt/^{195}Pt$ and $^{196}Pt/^{195}Pt$ are denoted $\delta^{198}Pt_{(8/5)}$ and $\delta^{198}Pt_{(6/5)}$, respectively. To assess the magnitude and importance of the correction for cosmogenic isotope effects, the $\delta^{198}Pt$ data that result if no such correction is applied are also reported as $\delta^{198}Pt_{(SRM)}$. The latter results are obtained if the isotope composition of SRM IRMM-010 Pt is applied as n instead of the unspiked isotope composition of the samples. Using the correction approach outlined above, the calculated $\delta^{198}Pt_{(8/5)}$ and $\delta^{198}Pt_{(6/5)}$ values are identical for all meteorites within error (Table 6).

With the exception of Tlacotepec, all iron meteorites analysed here have $\delta^{198}Pt_{(SRM)}$ results that are identical to the $\delta^{198}Pt_{(8/5)}$ and $\delta^{198}Pt_{(6/5)}$ values given the analytical uncertainties. In contrast, the $\delta^{198}Pt_{(8/5)}$ and $\delta^{198}Pt_{(6/5)}$ data for Tlacotepec were corrected for cosmogenic isotope effects of +0.11 and +0.13‰, respectively. The magnitude of the corrections, particularly relative to the spread of $\delta^{198}Pt$ values observed for the irons, show that they are significant and will need to be considered in any future high-precision studies of mass-dependent Pt isotope compositions for iron meteorites.

As the cosmogenic isotope effects for ^{194}Pt are dominated by the burnout of ^{193}Ir,[3] the Ir/Pt ratio has a critical impact on the GCR-induced isotope anomalies of all Pt isotope ratios that are employed in the double spike data reduction ($^{195}Pt/^{194}Pt$, $^{196}Pt/^{194}Pt$ and $^{198}Pt/^{194}Pt$) and therefore also on the calculated $\delta^{198}Pt$ values. The combined cosmogenic isotope effects for each of these ratios will therefore be a function of both the chemical compositions (Ir/Pt ratio) and the extent of exposure to GCR, and these parameters will vary between samples. For instance, Bendego 2 has $\delta^{198}Pt$ values that are identical for the corrected ($\delta^{198}Pt_{(8/5)}$, $\delta^{198}Pt_{(6/5)}$) and uncorrected results ($\delta^{198}Pt_{(SRM)}$), even though this sample exhibits cosmogenic

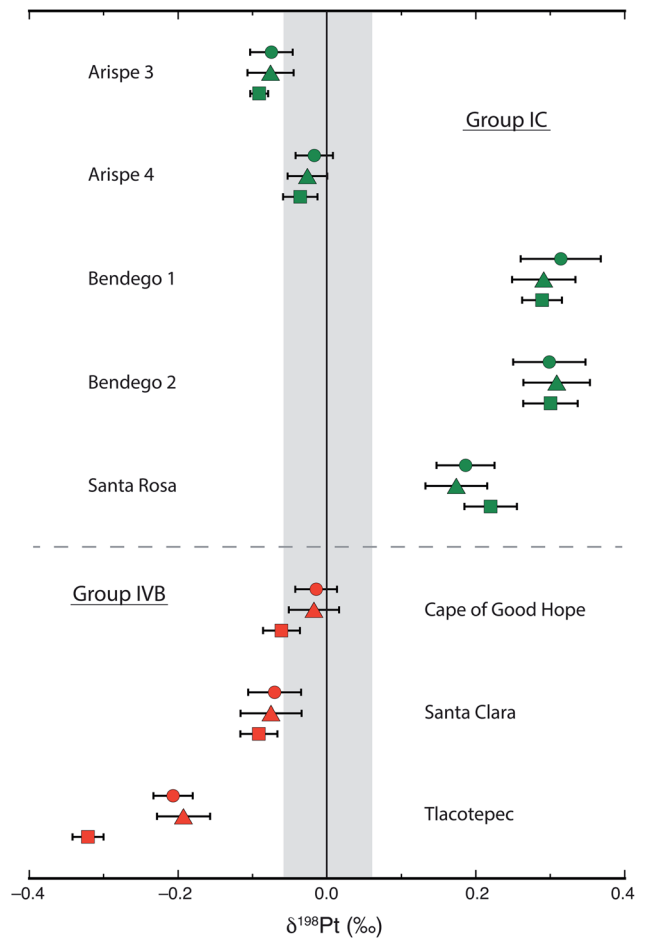

Fig. 8 $\delta^{198}Pt$ values of iron meteorites. Circles = $\delta^{198}Pt_{(8/5)}$, triangles = $\delta^{198}Pt_{(6/5)}$, squares = $\delta^{198}Pt_{(SRM)}$. Uncertainties are propagated 2se = $2\sigma/\sqrt{n}$, where n is the number of sample analyses.

isotope effects of a similar magnitude to Tlacotepec in $\varepsilon^{196}Pt_{(8/5)}$, with results of 0.96 ± 0.02 and 0.89 ± 0.06, respectively (Tables 4 and 6). However, Bendego 2 displays a much lower cosmogenic isotope anomaly for $\varepsilon^{194}Pt_{(8/5)}$ than Tlacotepec, with values of 1.20 ± 0.19 and 2.11 ± 0.11, respectively. The different extents of the cosmogenic isotope anomalies of Bendego 2 and Tlacotepec for $\varepsilon^{194}Pt_{(8/5)}$ *versus* $\varepsilon^{196}Pt_{(8/5)}$ is thereby well explained by the much lower Ir/Pt ratio of the former sample (0.02) relative to the latter (1.29; Table 6).

The contribution of cosmogenic isotope effects to the $\delta^{198}Pt_{(SRM)}$ values determined with the double spike technique are controlled by several factors, including exposure age, chemical composition, pre-atmospheric meteoroid radius and shielding depth, which will be unique for a specific sample aliquot. In accord with this conclusion, a previous study found that δ^{198}Pt data uncorrected for isotope anomalies induced by GCR exposure were poorly reproducible for some iron meteorites, including for replicate digestions of the same meteorite, and these problems were attributed to variable cosmogenic isotope effects.[10] It is therefore paramount that accurate measurements of mass-dependent Pt isotope compositions utilise sample aliquot specific corrections of cosmogenic isotope effects and the methods presented here provide an efficient and effective approach to achieve this.

Intriguingly, our pilot analyses reveal variations in mass-dependent Pt isotope composition both within and between different groups of iron meteorites, whereby the $\delta^{198}Pt_{(8/5)}$ values of the IC and IVB irons range from −0.07 to +0.31‰ and −0.21 to −0.01‰, respectively. This suggests that use of our methods to study the mass-dependent Pt isotope compositions of iron meteorites may provide novel constraints on planetary processes, such as core formation and subsequent core cooling and crystallisation.

Conclusions

This study presents new and improved analytical procedures for the determination of both the mass-independent and mass-dependent Pt isotope compositions of iron meteorites. In particular, our method for the separation of Pt is superior to published procedures in terms of sample throughput, Pt yield and the purity of the separated Pt fractions, which enable isotope analyses with no significant interferences from molecular ions or matrix effects. In combination with our MC-ICP-MS measurement routine, this enables the precise acquisition of mass-independent Pt isotope data with internal normalisation of the instrumental mass bias. Such data are of interest to obtain sample aliquot specific constraints on the cosmogenic isotope effects induced by exposure to GCR, as these can be used to correct the correlated anomalies of other affected isotope systems to accurate 'pre-exposure' values.

Also presented is a new procedure for precise determination of mass-dependent Pt isotope compositions that employs a double spike and MC-ICP-MS. Pilot results obtained for iron meteorites reveal the importance of correcting for cosmogenic Pt isotope effects to obtain unbiased δ^{198}Pt data from the double spike data reduction. It is furthermore shown that the mass-dependent Pt isotope compositions determined for unspiked samples provide sample aliquot specific neutron dosimetry, which can be applied in the data reduction to correct for Pt isotope effects induced by exposure to GCR. This procedure yields accurate mass-dependent Pt isotope compositions for iron meteorites with variable compositions and exposure ages. The initial results of this study reveal significant variations of δ^{198}Pt within and between iron meteorite groups, which suggests that such analyses might yield valuable data for studies of planetary processes.

Author contributions

MR and GP conceived the study. GP and RS undertook the laboratory and mass spectrometry work. GP and MR developed the data reduction methods, the interpretation of the data and wrote the manuscript. RS contributed to the development of the analytical methods.

Conflicts of interest

The authors declare no competing interests.

Acknowledgements

We thank R. Ickert and a second reviewer for their constructive and thorough reviews, and K. Hall for editorial handling. We are indebted to Barry Coles, Katharina Kreissig and the MAGIC group for help with analytical work. Caroline Smith and Deborah Cassey (The Natural History Museum, London) are recognised for assistance in selecting and providing meteorite specimens. The project was supported by an STFC studentship to GP and a research grant from STFC to MR (ST/J001260/1). GP was supported at Bristol by NERC grant NE/M000419/1.

References

1 T. S. Kruijer, M. Fischer-Gödde, T. Kleine, P. Sprung, I. Leya and R. Wieler, *Earth Planet. Sci. Lett.*, 2013, **361**, 162–172.
2 A. C. Hunt, M. Ek and M. Schönbächler, *Geochim. Cosmochim. Acta*, 2017, **216**, 82–95.
3 I. Leya and J. Masarik, *Meteorit. Planet. Sci.*, 2013, **48**, 665–685.
4 R. J. Walker, *Earth Planet. Sci. Lett.*, 2012, **351**, 36–44.
5 M. Fischer-Gödde and T. Kleine, *Nature*, 2017, **541**, 525–527.
6 T. S. Kruijer, M. Touboul, M. Fischer-Gödde, K. R. Bermingham, R. J. Walker and T. Kleine, *Science*, 2014, **344**, 1150–1154.
7 M. Ek, A. C. Hunt, M. Lugaro and M. Schönbächler, *Nat. Astron.*, 2020, **4**, 273–281.
8 E. A. Worsham, K. R. Bermingham and R. J. Walker, *Earth Planet. Sci. Lett.*, 2017, **467**, 157–166.
9 L. Qin, N. Dauphas, M. F. Horan, I. Leya and R. W. Carlson, *Geochim. Cosmochim. Acta*, 2015, **153**, 91–104.
10 J. B. Creech, J. A. Baker, M. R. Handler, J. P. Lorand, M. Storey, A. N. Wainwright, A. Luguet, F. Moynier and M. Bizzarro, *Geochemical Perspectives Letters*, 2017, **3**, 94–104.

11 F. Spitzer, C. Burkhardt, G. Budde, T. S. Kruijer, A. Morbidelli and T. Kleine, *Astrophys. J.*, 2020, **898**, L2.
12 R. M. G. Armytage, R. B. Georg, P. S. Savage, H. M. Williams and A. N. Halliday, *Geochim. Cosmochim. Acta*, 2011, **75**, 3662–3676.
13 F. Moynier, Q.-Z. Yin and E. Schauble, *Science*, 2011, **331**, 1417–1420.
14 C. Burkhardt, R. C. Hin, T. Kleine and B. Bourdon, *Earth Planet. Sci. Lett.*, 2014, **391**, 201–211.
15 K. Murphy, M. Rehkämper, K. Kreissig, B. Coles and T. van de Flierdt, *J. Anal. At. Spectrom.*, 2016, **31**, 319–327.
16 G. M. Poole, M. Rehkämper, B. J. Coles, T. Goldberg and C. L. Smith, *Earth Planet. Sci. Lett.*, 2017, **473**, 215–226.
17 J. F. Rudge, B. C. Reynolds and B. Bourdon, *Chem. Geol.*, 2009, **265**, 420–431.
18 M. Klaver and C. D. Coath, *Geostand. Geoanal. Res.*, 2019, **43**, 5–22.
19 M. Rehkämper and A. N. Halliday, *Talanta*, 1997, **44**, 663–672.
20 J. B. Creech, J. A. Baker, M. R. Handler and M. Bizzarroc, *Chem. Geol.*, 2014, **363**, 293–300.
21 A. C. Hunt, M. Ek and M. Schönbächler, *Geostand. Geoanal. Res.*, 2017, **41**, 633–647.
22 T. S. Kruijer, C. Burkhardt, G. Budde and T. Kleine, *Proc. Natl. Acad. Sci. U. S. A.*, 2017, **114**, 6712–6716.
23 M. Gault-Ringold and C. H. Stirling, *J. Anal. At. Spectrom.*, 2012, **27**, 449–459.
24 M. Berglund and M. E. Wieser, *Pure Appl. Chem.*, 2011, **83**, 397–410.
25 E. D. Young, A. Galy and H. Nagahara, *Geochim. Cosmochim. Acta*, 2002, **66**, 1095–1104.
26 J. Creech, J. Baker, M. Handler, M. Schiller and M. Bizzarro, *J. Anal. At. Spectrom.*, 2013, **28**, 853–865.
27 F. Wombacher and M. Rehkämper, *J. Anal. At. Spectrom.*, 2003, **18**, 1371–1375.
28 S. Ripperger and M. Rehkämper, *Geochim. Cosmochim. Acta*, 2007, **71**, 631–642.
29 C. Siebert, T. F. Nagler and J. D. Kramers, *Geochem., Geophys., Geosyst.*, 2001, **2**, 2000GC000124.
30 Z. Xue, M. Rehkämper, T. J. Horner, W. Abouchami, R. Middag, T. van de Flierdt and H. J. W. de Baar, *Earth Planet. Sci. Lett.*, 2013, **382**, 161–172.
31 J. Y. Hu and N. Dauphas, *J. Anal. At. Spectrom.*, 2017, **32**, 2024–2033.
32 T. Hopp, M. Fischer-Gödde and T. Kleine, *Geochim. Cosmochim. Acta*, 2018, **223**, 75–89.
33 B. L. A. Charlier, I. J. Parkinson, K. W. Burton, M. M. Grady, C. J. N. Wilson and E. G. C. Smith, *Geochemical Perspectives Letters*, 2017, **4**, 35–40.
34 E. A. Worsham, C. Burkhardt, G. Budde, M. Fischer-Gödde, T. S. Kruijer and T. Kleine, *Earth Planet. Sci. Lett.*, 2019, **521**, 103–112.
35 S. J. G. Galer, *Chem. Geol.*, 1999, **157**, 255–274.